Bloch–Zener quantum walk

2012 J. Phys. B: At. Mol. Opt. Phys. 45 225504

(http://iopscience.iop.org/0953-4075/45/22/225504)

J. Phys. B: At. Mol. Opt. Phys. **45** (2012) 225504 (8pp) doi:10.1088/0953-4075/45/22/225504

Bloch–Zener quantum walk

S Longhi

Dipartimento di Fisica, Politecnico di Milano and Istituto di Fotonica e Nanotecnologie del Consiglio Nazionale delle Ricerche, Piazza L da Vinci 32, I-20133 Milano, Italy

E-mail: longhi@fisi.polimi.it

Received 25 July 2012, in final form 29 August 2012
Published 8 November 2012
Online at stacks.iop.org/JPhysB/45/225504

Abstract
Coherent transport of quantum particles in binary superlattices driven by an *ac force* can realize a kind of quantum walk (QW) that can be referred to as Bloch–Zener QW. In this regime, the particle wavepacket undergoes a sequence of Zener tunnelling events that mimic a discrete QW on a lattice, provided that the impulse of the ac force over one semi-cycle of oscillation is properly adjusted. In the Bloch–Zener QW, the coin states are related to the particle occupation of the two minibands, and thus it does not require any internal degrees of freedom of the particle.

(Some figures may appear in colour only in the online journal)

1. Introduction

Coherent transport of quantum particles in a periodic potential is crucially influenced by the lattice band structure. One of the most striking examples is provided by the well-known Bloch oscillations (BOs): a particle in a static crystalline potential subjected to a dc force undergoes an oscillatory rather than a uniformly accelerated motion [1]. BOs have been observed in a wide variety of physical systems, including semiconductor superlattices [2], ultracold atoms and Bose–Einstein condensates [3–5], photonic lattices [6–8] and acoustic crystals [9]. Coherent transport under an ac force has been generally related to the phenomenon of dynamic localization [10–18], i.e. suppression of quantum spreading in the lattice. Interestingly, a pure ac force, or a combined ac–dc force, can realize a directed transport [19, 20]. Directed transport under a dc force can be realized as well for vibrating lattices [21]. In a binary superlattice, a single band is split into two minibands, and Zener tunnelling (ZT) between them makes coherent transport more involved. The application of a dc force leads to a sequence of BOs and ZT transitions that organize to give the so-called Bloch–Zener oscillations (BZOs) [22–27]. BZOs have been recently observed for both optical [28] and matter waves [29]. In BZOs, the avoided crossing between the two minibands acts as a coherent beam splitter for a particle wavepacket, which is responsible for interference effects at both single- and multiple-particle levels [30].

In this work we predict a novel regime of coherent quantum transport for spinless particles moving on a binary superlattice and subjected to an *ac force* that can be referred to as Bloch–Zener quantum walk (BZQW). In this regime, the particle wavepacket undergoes a discrete QW [31, 32] as a result of an organized sequence of ZT events. QWs have been the subject of extensive investigations in the past decade, with major impact in different fields, for instance, in quantum information science or in the transport properties of biomolecules. Realizations of QWs have been proposed and reported in several physical systems, including nuclear magnetic resonance systems [33], optical trapped ions [34, 35] and atoms [36], and photonic networks [37–46]. QWs based on Landau–Zener transitions in multilevel systems have been suggested in [47]. For trapped ions or atoms in optical lattices, QWs generally require some internal degrees of the particle (such as spin) to implement the coin states and/or special procedures with controlled fields to shift the particle (see, for instance, [20, 34–36, 48–52]). In the BZQW proposed in this work, the particle undergoing the QW does not need to have any internal degrees of freedom nor is dynamic control of the lattice potential required. However, the unit cell of the superlattice comprises two wells and the superlattice thus sustains two minibands, which play the roles of the coin states and basically replace the internal degree of freedom (e.g. spin) of the particle.

2. Bloch–Zener oscillations and quantum walk

Let us consider a single particle of mass m moving on a one-dimensional binary superlattice driven by an external ac force $F(t)$ with period $T = 2\pi/\omega$. The particle motion is governed by the Schrödinger equation

$$\mathrm{i}\partial_t \psi = \hat{H}\psi = \hat{H}_0\psi - F(t)x\psi \qquad (1)$$

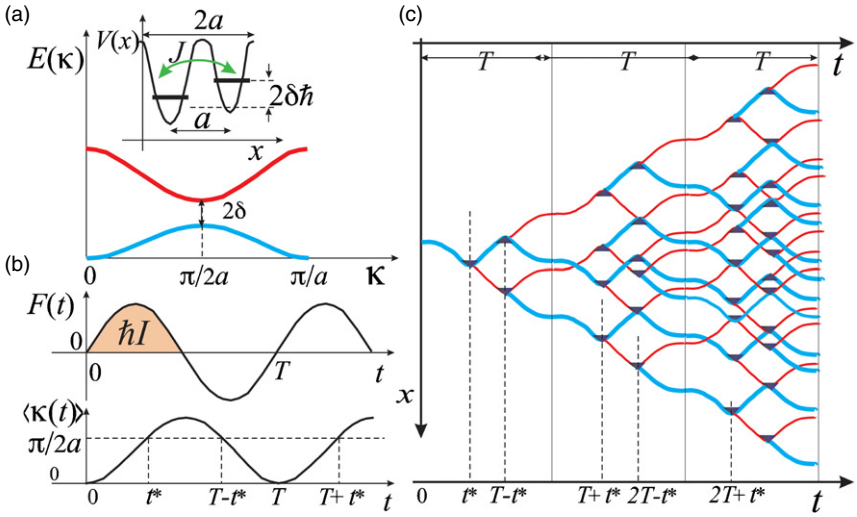

Figure 1. (a) Band diagram of a binary superlattice; the inset shows the unit cell of the lattice. (b) Plots of the ac force $F(t)$ and of the Bloch wave number $\langle\kappa(t)\rangle$ as obtained by the semiclassical analysis. ZT occurs at times such that $\kappa = \pi/(2a)$. (c) Sequence of wavepacket splitting induced by ZT and paths followed by the split wavepackets as predicted by the semiclassical analysis. Thick solid (blue) curves refer to wavepackets belonging to the lower miniband, whereas thin solid (red) curves refer to wavepackets belonging to the upper miniband. Triangles in the graph show the splitting regions (nodes) due to ZT.

for the amplitude wavefunction $\psi(x,t)$, where $\hat{H}_0 = -(\hbar^2/2m)\partial_x^2 + V(x)$ and $V(x)$ is the lattice potential, which is assumed to be periodic with period $2a$. The unit cell of the lattice comprises two slightly different wells spaced by a (see the inset of figure 1(a)). In this way the two lowest energy minibands, separated by a small gap, arise in the energy spectrum of $\hat{H}_0$ (see figure 1(a)). In the framework of a two-band model, the particle wavepacket ψ can be decomposed as a superposition of two wavepackets ψ_1 and ψ_2 belonging to the two minibands, i.e. $\psi(x,t) = \psi_1(x,t) + \psi_2(x,t)$ (see the appendix for the technical details). A simple picture of the wavepacket motion can be gained in the framework of a semiclassical analysis [1]. Indicating by $\langle x_{1,2}\rangle(t)$ the mean positions of wavepackets $\psi_1(x,t)$ and $\psi_2(x,t)$ and by $\hbar\langle\kappa(t)\rangle$ the mean particle quasi-momentum, the semiclassical equations of motion read [1]

$$\hbar\frac{d\langle\kappa\rangle}{dt} = F(t), \qquad \hbar\frac{d\langle x_{1,2}\rangle}{dt} \simeq \frac{\partial E_{1,2}}{\partial\kappa}(\langle\kappa\rangle), \tag{2}$$

where $E_{1,2}(\kappa)$ are the dispersion curves of the two minibands. The ac force is assumed to satisfy the symmetry condition $F(-t) = -F(t)$ and to have a definite sign (either positive or negative) in each semi-cycle of oscillation (for instance, $F(t) > 0$ for $0 < t < T/2$ and $F(t) < 0$ for $T/2 < t < T$). Such conditions apply e.g. to a sinusoidal $[F(t) = F_0\sin(\omega t)]$ or to a square-wave force. Moreover, we will assume that $\pi/(2a) < I < 3\pi/(2a)$, where $\hbar I \equiv \int_0^{T/2} F(t)\,dt$ is the impulse of the force in the (positive) semi-cycle of oscillation. In this way, assuming that the initial wavepacket is at rest (i.e. $\langle\kappa(0)\rangle = 0$), the quasi-momentum $\langle\kappa(t)\rangle$, as obtained by equation (2), is a periodic function of time and bounded in the range $[0, 3\pi/(2a)]$ (see figure 1(c)). ZT between the two minibands, and thus mixing of the wavepackets ψ_1 and ψ_2, occurs whenever $\langle\kappa(t)\rangle$ reaches the boundary of the Brillouin zone, i.e. at times t such that $\langle\kappa(t)\rangle = \pi/(2a)$. In each oscillation cycle, this happens twice at times t^* and $T - t^*$, as shown in figure 1(b). Note that, for a sinusoidal or square-wave forces, one has $t^* = T/4$. Let us now assume that at the initial time, the particle wavepacket $\psi(x,0)$ belongs to the lower miniband; the path followed by this wavepacket is thus governed by equation (2), taking $E_1(\kappa)$ for the band dispersion curve. At $t = t^*$, ZT occurs and a fraction of the wavepacket tunnels into the upper miniband and follows a different path, obtained from equation (2) taking $E_2(\kappa)$ for the dispersion curve. In real space, at around $t = t^*$, $\psi(x,t)$ is thus split into two parts, i.e. ZT acts as a coherent beam splitter (BS). At $t = T - t^*$, a second ZT occurs. Provided that the two wavepacket parts are spatially separated at the second ZT, a further splitting occurs, i.e. the initial wavepacket is split into four parts, two belonging to the lower minibands and the other two to the upper minibands. In this way, a sequence of beam splitting in real space occurs at the ZT times $t_1 = t^*$, $t_2 = T - t^*$, $t_3 = t^* + T$, $2T - t^*$, ... The paths followed by the various split wavepackets, belonging to either the lower or upper minibands and computed using equation (2), generate a graph with nodes at the ZT times, as shown in figure 1(c). Since the split wavepackets do not generally recombine at the successive ZT times, the number of nodes at a crossing time t_n is larger than n; see figure 1(c) as an example. However, if the condition $I = \pi/a$ is satisfied, wavepacket recombination occurs regularly, as shown in figure 2(a). In this case, the graph has exactly n nodes at time t_n, i.e. the sequence of ZT events acts as a chain of BS in the tree scheme, as shown in figure 2(b). Note that the condition $I = \pi/a$ corresponds to the absence of directed transport of the particle in either one of the two minibands, i.e. in this case one has $x_{1,2}(nT) = x_{1,2}(0)$ according to the semiclassical equations (2). The motion of the particle undergoing the sequence of ZT along the tree basically realizes a discrete QW. In fact, let us introduce the discrete times $\tau_m = mT/2$ $(m = 0, 1, 2, \ldots)$ and let us indicate by $\{a_n(\tau_m), b_n(\tau_m)\}$ the amplitudes of the wavepackets at time τ_m, belonging to the lower and upper minibands, respectively,

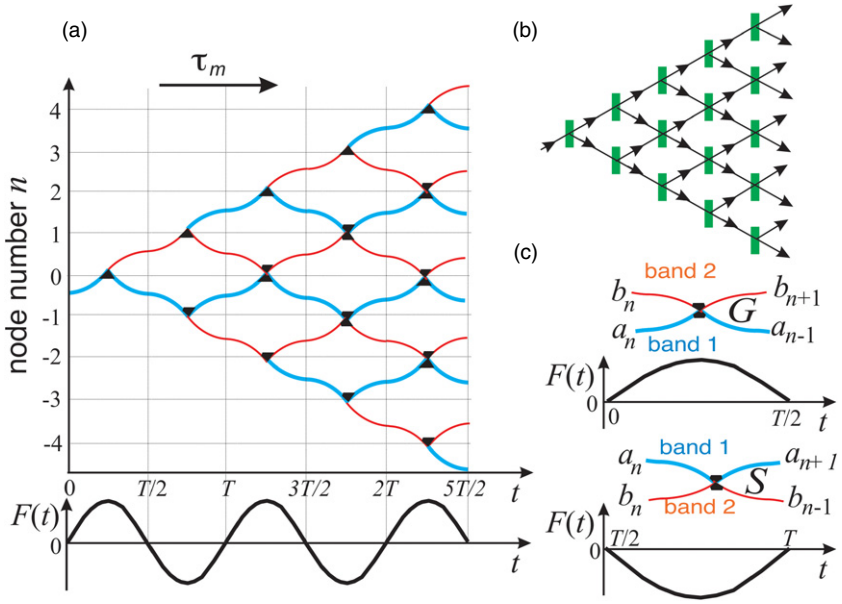

Figure 2. (a) Paths followed by the split wavepackets, as predicted by the semiclassical equations, for an ac force with $I = \pi/a$. The graph is equivalent to the tree of BS shown in (b), where at each node ZT acts as the BS in the tree. Wavepacket splitting and recombination at the ZT times are described by the scattering matrices G and S in the two semi-cycles of oscillations, as shown in (c).

that are flowing towards the nth node in the graph (see figure 2(a)). From the path followed by the various wavepackets, as shown in figure 2(a), the following recursive relations can be obviously written:

$$a_n(\tau_{m+1}) = G_{11}a_{n+1}(\tau_m) + G_{12}b_{n+1}(\tau_m) \tag{3}$$

$$b_n(\tau_{m+1}) = G_{21}a_{n-1}(\tau_m) + G_{22}b_{n-1}(\tau_m) \tag{4}$$

for m even, and

$$a_n(\tau_{m+1}) = S_{11}a_{n-1}(\tau_m) + S_{12}b_{n-1}(\tau_m) \tag{5}$$

$$b_n(\tau_{m+1}) = S_{21}a_{n+1}(\tau_m) + S_{22}b_{n+1}(\tau_m) \tag{6}$$

for m odd, where G and S are the (unitary) scattering matrices that describe ZT in the two semi-cycles $(0, T/2)$ and $(T/2, T)$ of the ac force, respectively, as schematically shown in figure 2(c). The determination of the scattering matrices S and G, which is detailed in the appendix, cannot be done in the framework of the simple semiclassical model and requires the knowledge of the Bloch–Floquet modes of the two minibands. After setting $x_n(\tau_m) = a_n(\tau_m)$, $y_n(\tau_m) = b_n(\tau_m)$ for m even, and $x_n(\tau_m) = b_n(\tau_m)$, $y_n(\tau_m) = a_n(\tau_m)$ for m odd, the following map is obtained for $\{x_n(\tau_m), y_n(\tau_m)\}$:

$$x_n(\tau_{m+1}) = C_{11}(\tau_m)x_{n-1}(\tau_m) + C_{12}(\tau_m)y_{n-1}(\tau_m) \tag{7}$$

$$y_n(\tau_{m+1}) = C_{21}(\tau_m)x_{n+1}(\tau_m) + C_{22}(\tau_m)y_{n+1}(\tau_m), \tag{8}$$

where we have introduced the time-dependent coin matrix $C(\tau_m)$ given by

$$C(\tau_m) = \begin{pmatrix} G_{21} & G_{22} \\ G_{11} & G_{12} \end{pmatrix} \ (m \text{ even}), \quad \begin{pmatrix} S_{12} & S_{11} \\ S_{22} & S_{21} \end{pmatrix} \ (m \text{ odd}). \tag{9}$$

In their present form equations (7) and (8) define a discrete QW on a lattice, with a time-dependent (alternating) coin matrix defined by equation (9) (see, for instance, [31, 32]). Note that the effect of the ac force is basically to periodically split and shift up or down an initial wavepacket. At each splitting the 'coin state' that rules the up or down shift is the miniband index $\alpha = 1, 2$. Hence, as compared to previous schemes of QWs of cold neutral atoms or ions trapped in optical lattices [20, 34–36, 48–52], the BZQW does not require any internal degrees of freedom of the particle nor the application of dynamic potentials or tailored control fields to shift the particle. Like in any discrete QW, the probability of finding the particle at time τ_m directed towards the node n of the graph arises from the interference among the different paths that the particle can follow, and can be computed as

$$P_n(\tau_m) = |a_n(\tau_m)|^2 + |b_n(\tau_m)|^2. \tag{10}$$

Let us finally note that the wavepacket splitting and recombination dynamics described above, which is basically equivalent to the sequence of beam splitters shown in figure 2(c), is a fully deterministic process. If we consider, as an example, a photonic realization of the BZQW using an array of coupled optical waveguides [28], the tree structure as shown in figure 2(a) can be reproduced deterministically by a classical (coherent state) light beam that undergoes BOs and Zener tunnelling as it propagates along the waveguide lattice. However, if we consider the single-photon excitation of the array, like in a conventional beam splitter at the Zener transition point the photon does not split, but follows either one of the two paths with a probability that is defined by the ZT matrix. Therefore a single photon undergoes a truly QW, the randomness being associated with the quantum nature of the problem and by the measure of an observer.

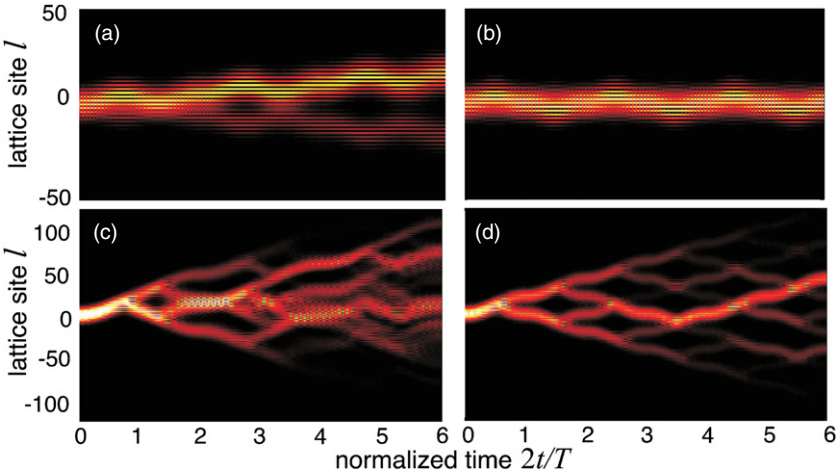

Figure 3. Numerically computed evolution of a Gaussian wavepacket (snapshot of $|c_l(t)|^2$) in a tight-binding lattice driven by a square-wave force for (a) $\delta/J = 3$, $T = 31/J$, and $F_0 = 0.7(\hbar\omega/a)$; (b) $\delta/J = 3$, $T = 31/J$, and $F_0 = (\hbar\omega/a)$; (c) $\delta/J = 0.3$, $T = 31/J$ and $F_0 = 0.7(\hbar\omega/a)$; and (d) $\delta/J = 0.3$, $T = 31/J$ and $F_0 = (\hbar\omega/a)$. The initial condition is $c_l(0) = \mathcal{N}\exp[-(l/\sigma)^2]$ with $\sigma = 9$.

3. Bloch–Zener quantum walk in a tight-binding superlattice

Let us specialize our analysis by considering a standard tight-binding model of a binary superlattice, which has been previously considered, both theoretically [22–24] and experimentally [28], to demonstrate the onset of BZOs under a dc force. For a single particle, the tight-binding Hamiltonian reads $\hat{H} = \hat{H}_0 - F(t)a\sum_l l|l\rangle\langle l|$, where

$$\hat{H}_0 = -J\hbar\sum_l (|l+1\rangle\langle l| + |l\rangle\langle l+1|) + \hbar\delta\sum_l (-1)^l |l\rangle\langle l|, \tag{11}$$

$|l\rangle$ is the Wannier state localized at the lth site of the lattice, $2\hbar\delta$ is the difference between the energy levels in two adjacent wells of the superlattice and J is the hopping rate (see figure 1(a)). After setting $|\psi(t)\rangle = \sum_l c_l(t)|l\rangle$, the occupation amplitudes $c_l(t)$ satisfy the coupled equations

$$\mathrm{i}\frac{\mathrm{d}c_l}{\mathrm{d}t} = -J(c_{l+1} + c_{l-1}) + (-1)^l\delta c_l - \frac{F(t)al}{\hbar}c_l. \tag{12}$$

For this model, the band dispersion curves, the Bloch–Floquet states and the ZT scattering matrices can be computed in a closed form (see the appendix). In particular, it can be shown that S is the transpose of G, i.e. $S = G^{\mathrm{T}}$. The ac force is chosen to be either sinusoidal $F(t) = F_0\sin(\omega t)$ or square-wave $F(t) = F_0 H(\omega t)$, where $H(t + 2\pi) = H(t)$, $H(t) = 1$ for $0 < t < \pi$ and $H(t) = -1$ for $\pi < t < 2\pi$. To realize a QW, the amplitude F_0 of the force must satisfy the condition $I = \pi/a$, i.e. $F_0 = \pi\hbar\omega/(2a)$ for the sinusoidal modulation and $F_0 = \hbar\omega/a$ for the square-wave modulation. Figure 3 shows, as examples, the evolution of $|c_l(t)|^2$, as obtained by a numerical analysis of equations (12), for a square-wave modulation when the lattice is initially excited by a broad wavepacket with the Gaussian distribution and zero mean momentum, $c_l(0) = \mathcal{N}\exp[-(l/\sigma)^2]$, where $\mathcal{N}$ is a normalization constant and $\sigma \gg 1$. This wavepacket basically excites only the lower miniband of the superlattice. In the absence of ZT, i.e. for a large value of δ, the wavepacket does not split and undergoes an oscillatory motion, with a directed transport when the impulse of the force $\hbar I$ is different than $\hbar\pi/a$, as shown in figures 3(a) and (b). When the gap width 2δ becomes of the same order of the hopping rate J, ZT comes into play and the wavepacket breaks up at the ZT times, as shown in figures 3(c) and (d). According to the semiclassical analysis, when $I \neq \pi/a$, the bifurcating paths followed by the particle at ZT times are rather irregular (see figure 3(c)), whereas for $I = \pi/a$ a regular graph is realized and the particle undergoes a discrete QW, as shown in figure 3(d). The corresponding evolution of the distribution probability $P_n(\tau_m)$ of the particle at the graph nodes n and at the discrete times $\tau_m = mT/2$ ($m = 0, 1, 2, 3, \ldots$), as obtained by the numerical analysis of the maps (7) and (8) with the coin matrix C as given by equation (9), is shown in figure 4(a). Parameter values have been chosen to have 50% probability of ZT at each crossing; obviously by tuning the values of detuning δ, hopping rate J and forcing F_0 different coin matrices (and thus probability distributions) can be realized. A correspondence between the evolution of $P_n(\tau_m)$ in the discrete lattice and the wavepacket evolution in the physical superlattice can be clearly seen. Note that, since the initial coin state is well defined ($\alpha = 1$), the probability distribution $P_n(\tau_m)$ is not symmetric around $n = 0$ and a preferential direction of motion is visible. This behaviour is a quite general feature of a QW and related to the initial state condition (see, for instance, [31]); a symmetric QW would be obtained when the initial coin state is in a balanced superposition of $\alpha = 0$ and $\alpha = 1$ states. By changing the initial coin state (from $\alpha = 1$ to $\alpha = 2$), the behaviour of $P_n(\tau_m)$ can be reversed, as shown in figure 4(b). In the figure, the initial wavepacket distribution is now $c_l(0) = \mathcal{N}(-1)^n\exp[-(l/\sigma)^2]$, which mainly excites the upper miniband of the superlattice. The above examples refer to a square-wave modulation; however, similar results are obtained for a sinusoidal force, as shown in the examples of figures 4(c) and (d).

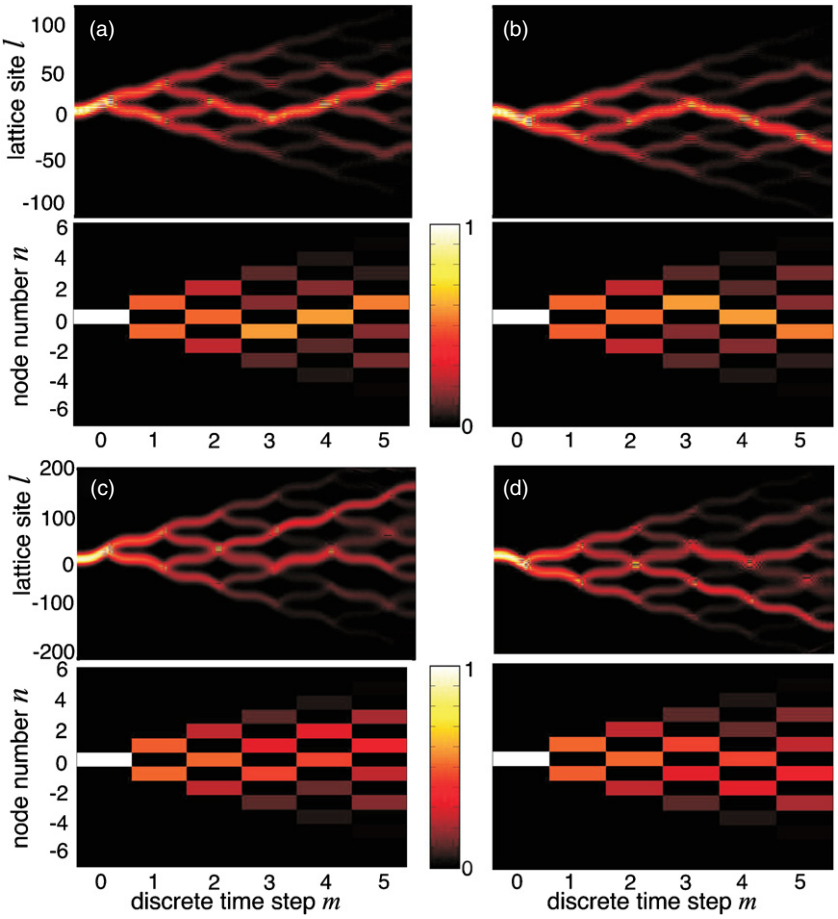

Figure 4. (a) and (b) Evolution of a Gaussian wavepacket (snapshot of $|c_l(t)|^2$) driven by a square-wave force for $\delta/J = 0.3$, $T = 31/J$, $F_0 = (\hbar\omega/a)$ and for the two initial conditions $c_l(0) = \mathcal{N}\exp[-(l/\sigma)^2]$ in (a), and $c_l(0) = \mathcal{N}(-1)^l\exp[-(l/\sigma)^2]$ in (b), with $\sigma = 9$. The lower panels in the figure show the evolution of the probability distribution $P_n(\tau_m)$ of the discrete QW as obtained by equations (7)–(10). (c) and (d) The same as (a) and (b), but for a sinusoidal force ($\delta/J = 0.235$, $T = 80/J$, $F_0 = \pi\hbar\omega/(2a)$, $\sigma = 15$).

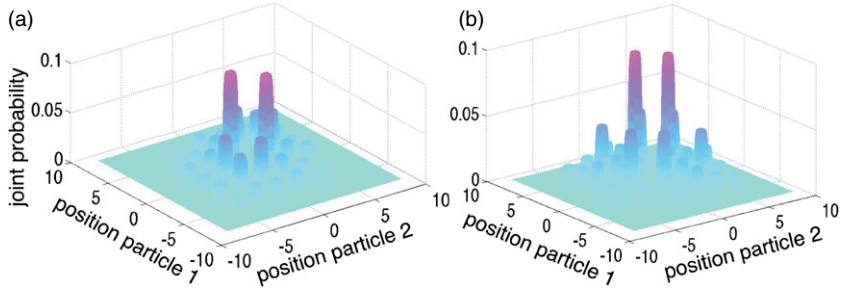

Figure 5. Joint probability $P_{n,l}$ for two indistinguishable particles undergoing BZQW under sinusoidal driving at the discrete time step $m = 7$ for (a) bosons and (b) fermions. Parameter values are as in figures 4(c) and (d).

4. Many-particle Bloch–Zener quantum walk

In the previous sections the analysis has been focused to a single-particle BZQW; however, the results can be extended to non-interacting many particles undergoing BZQW (see, for instance, [30]). In this case, entanglement between the particles introduces new features into the QW, which depend on the statistics of the particles [53]. Let us consider, for instance, the coherent transport of two indistinguishable and non-interacting particles. In the framework of the tight-binding model, the two-particle wavefunction is given by

$$|\psi(t)\rangle = \sum_{l,s}(1/\sqrt{2})c_l(t)v_s(t)\,(|l\rangle_1|s\rangle_2 \pm |l\rangle_2|s\rangle_1)\,, \qquad (13)$$

where $c_l(t)$ and $v_s(t)$ are the single-particle occupation amplitudes that satisfy equation (12) with the appropriate initial conditions, and the plus (minus) sign holds for bosonic (fermionic) particles. As an initial condition let us assume, $c_l(0) = \mathcal{N}\exp(-l^2/\sigma^2)$ and $v_s(0) = (-1)^s\mathcal{N}\exp[-(s - s_0)^2/\sigma^2]$, corresponding to one particle exciting the lower miniband of the superlattice, the other particle the upper

miniband of the superlattice (see figure 4), with a spatial offset s_0 such that the two wavepackets cross at the first ZT time t^*. Let us indicate by $\{a_n, b_n\}$ and by $\{A_n, B_n\}$ the single-particle QW at some discrete time τ_m for the two different initial conditions. Then it can be readily shown that the joint probability $P_{n,j}(\tau_m)$ of finding one particle at node n and the other particle at node j is given by

$$P_{n,j} = \tfrac{1}{2}\left(P_n^{(1)}P_j^{(2)} + P_j^{(1)}P_n^{(2)}\right) \pm \mathrm{Re}(\Phi), \tag{14}$$

where $P_n^{(1)} = |a_n|^2 + |b_n|^2$, $P_j^{(2)} = |A_j|^2 + |B_j|^2$ are the one-particle probability distributions and $\Phi = (A_j a_j^* + B_j b_j^*)(a_n A_n^* + b_n B_n^*)$ accounts for quantum interference. As an example, figure 5 shows the bosonic and fermionic distributions of the joint probability $P_{n,j}$ at $m = 7$ and for the sinusoidal force of figures 4(c) and (d).

5. Conclusion

In conclusion, the coherent motion of quantum particles in a binary superlattice driven by an ac force can realize a QW as a result of an organized sequence of ZT events. This shows that ac forces can be exploited not only to reduce or suppress quantum diffusion [10–18], but also to realize a discrete QW. Our results may be of relevance to both matter-wave [29] and photonic [28] systems, paving the way towards further investigations of complex single- and many-particle coherent transport phenomena in driven lattice systems.

Appendix

1. Wave packet motion in a binary superlattice: ZT and scattering matrices. Let us indicate by $\phi_\alpha(x,\kappa) = u_\alpha(x,\kappa)\exp(\mathrm{i}\kappa x)$ the Bloch–Floquet eigenfunction of $\hat{H}_0$, corresponding to the αth lattice band and to wave number κ, with periodic part $u_\alpha(x,\kappa)$, i.e. $u_\alpha(x+2a,\kappa) = u_\alpha(x,\kappa)$. The wave number κ is assumed to vary in the interval $0 < \kappa \leqslant \pi/a$. Thus, $\hat{H}_0\phi_\alpha(x,\kappa) = E_\alpha(\kappa)\phi_\alpha(x,\kappa)$, where $E_\alpha(\kappa)$ is the dispersion curve of the αth band and $\phi_\alpha(x,\kappa)$ satisfy the orthonormal relations $\langle\phi_\beta(x,\kappa')|\phi_\alpha(x,\kappa)\rangle = \delta_{\alpha,\beta}\delta(\kappa-\kappa')$.

To study the coherent motion of a quantum particle in the lattice under external driving, we expand the wavepacket amplitude $\psi(x,t)$ as a superposition of Bloch–Floquet states belonging to the various lattice bands [1]. In this way, the wavepacket $\psi(x,t)$ can be viewed as arising from the superposition (interference) of wavepackets $\psi_1(x,t)$, $\psi_2(x,t)$, $\psi_3(x,t)$, ... belonging to the various lattice bands, namely one can write

$$\psi(x,t) = \psi_1(x,t) + \psi_2(x,t) + \psi_3(x,t) + \cdots, \tag{A.1}$$

where $\psi_\alpha(x,t)$ is given by the superposition of Bloch–Floquet states of the αth band. After setting

$$\psi_\alpha(x,t) = \sum_\alpha \int_0^{\pi/a} \mathrm{d}\kappa\, c_\alpha(\kappa,t)\phi_\alpha(\kappa,x), \tag{A.2}$$

the evolution of the spectral amplitudes $c_\alpha(\kappa,t)$ are governed by the coupled equations [1, 25]

$$\mathrm{i}\hbar\left(\frac{\partial}{\partial t} + \frac{F(t)}{\hbar}\frac{\partial}{\partial\kappa}\right)c_\alpha = E_\alpha(\kappa)c_\alpha - F(t)\sum_\beta X_{\alpha,\beta}(\kappa)c_\beta, \tag{A.3}$$

where

$$X_{\alpha,\beta}(\kappa) \equiv \frac{\mathrm{i}\pi}{a}\int_0^{2a}\mathrm{d}x u_\alpha^*(x,\kappa)\frac{\partial u_\beta(x,\kappa)}{\partial\kappa}. \tag{A.4}$$

Note that $X_{\beta,\alpha}(\kappa) = X_{\alpha,\beta}^*(\kappa)$. The off-diagonal elements $X_{\alpha,\beta}$ ($\alpha \neq \beta$) in equation (A.3) are responsible for interband transitions, i.e. Zener tunnelling. In a two-band model, which applies to a binary superlattice, we can restrict the analysis by considering only the two lowest minibands $\alpha = 1, 2$. Let us further assume that at initial time $t = 0$ the spectral coefficients $c_{1,2}$ are of the form $c_{1,2}(\kappa,0) = f_{1,2}(0)g(\kappa)$, where $g(\kappa)$ is narrow at around $\kappa = 0$ with the normalization $\int \mathrm{d}\kappa\, g(\kappa) = 1$. Such an assumption holds, as an example, for an initial slowly varying wavepacket $\psi(x,0)$ with zero mean momentum and spatially extended over several lattice sites. In this case, the lowest miniband of the superlattice is mainly excited, and one has $f_1(0) \simeq 1$, $f_2(0) \simeq 0$. An approximate solution to equation (A.3) is then given by

$$c_{1,2}(\kappa,t) \simeq f_{1,2}(t)\, g\left(\kappa - \frac{1}{\hbar}\int_0^t \mathrm{d}\xi F(\xi)\right), \tag{A.5}$$

where the amplitudes $f_{1,2}(t)$ evolve according to the coupled equations:

$$\begin{aligned}\mathrm{i}\hbar\frac{\mathrm{d}f_1}{\mathrm{d}t} = &\left[E_1\left(\frac{1}{\hbar}\int_0^t \mathrm{d}\xi F(\xi)\right)\right.\\ &\left. - F(t)X_{1,1}\left(\frac{1}{\hbar}\int_0^t \mathrm{d}\xi F(\xi)\right)\right]f_1(t)\\ &- F(t)X_{1,2}\left(\frac{1}{\hbar}\int_0^t \mathrm{d}\xi F(\xi)\right)f_2(t)\end{aligned} \tag{A.6}$$

$$\begin{aligned}\mathrm{i}\hbar\frac{\mathrm{d}f_2}{\mathrm{d}t} = &\left[E_2\left(\frac{1}{\hbar}\int_0^t \mathrm{d}\xi F(\xi)\right)\right.\\ &\left. - F(t)X_{2,2}\left(\frac{1}{\hbar}\int_0^t \mathrm{d}\xi F(\xi)\right)\right]f_2(t)\\ &- F(t)X_{2,1}\left(\frac{1}{\hbar}\int_0^t \mathrm{d}\xi F(\xi)\right)f_1(t)\end{aligned} \tag{A.7}$$

with the assigned initial conditions $f_{1,2}(0)$. For an ac force satisfying the conditions given in the text, in one oscillation cycle $(0,T)$ ZT occurs at the two times t^* and $T - t^*$ (see figure 1(b) given in the text), i.e. wavepacket splitting occurs twice, one in the first semi-cycle $(0, T/2)$ and the other one in the second semi-cycle $(T/2, T)$. We can then introduce two scattering matrices G and S that describe wavepacket splitting at the two ZT steps according to the relations (see figure 2(c) given in the text)

$$\begin{pmatrix} f_1\left(\frac{T}{2}\right)\\ f_2\left(\frac{T}{2}\right)\end{pmatrix} = G\begin{pmatrix} f_1(0)\\ f_2(0)\end{pmatrix}, \qquad \begin{pmatrix} f_1(T)\\ f_2(T)\end{pmatrix} = S\begin{pmatrix} f_1\left(\frac{T}{2}\right)\\ f_2\left(\frac{T}{2}\right)\end{pmatrix}. \tag{A.8}$$

The determination of the scattering matrices G and S can be generally done by the numerical analysis of equations (A.6) and (A.7) once the miniband Bloch–Floquet modes have been calculated.

2. Tight-binding binary superlattice. Let us specialize the previous analysis to a tight-binding binary superlattice, defined

by the Hamiltonian $\hat{H}_0$ and given by equation (6) in the text. In this case the dispersion curves of the two minibands can be readily calculated in a closed form and read $E_1(\kappa) = -\hbar\epsilon(\kappa)$, $E_2(\kappa) = -E_1(\kappa)$, where we have set

$$\epsilon(\kappa) = \sqrt{\delta^2 + 4J^2\cos^2(\kappa a)}. \tag{A.9}$$

Note that the width of the energy gap is $2\delta\hbar$. The Bloch–Floquet states $|\phi_{1,2}(\kappa)\rangle$ of the two minibands are then given by

$$|\phi_{1,2}(\kappa)\rangle = A_{1,2}(\kappa)\sum_l \exp(2\mathrm{i}\kappa a l)|2l\rangle + B_{1,2}(\kappa)\sum_l \exp[\mathrm{i}(2l+1)\kappa a]|2l+1\rangle, \tag{A.10}$$

where we have set

$$A_1(\kappa) = -\sqrt{\frac{a}{\pi}}\frac{2J\cos(\kappa a)}{\sqrt{4J^2\cos^2(\kappa a) + [\delta + \epsilon(\kappa)]^2}} \tag{A.11}$$

$$B_1(\kappa) = -\sqrt{\frac{a}{\pi}}\frac{\delta + \epsilon(\kappa)}{\sqrt{4J^2\cos^2(\kappa a) + [\delta + \epsilon(\kappa)]^2}} \tag{A.12}$$

$$A_2(\kappa) = -B_1(\kappa), \qquad B_2(\kappa) = A_1(\kappa). \tag{A.13}$$

The spectral coefficients $X_{\alpha,\beta}(\kappa)$ $(\alpha, \beta = 1, 2)$ entering in the spectral equations (A.6) and (A.7) can be calculated from equation (A.4) using equation (A.10). One obtains

$$X_{\alpha,\beta}(\kappa) = \frac{\mathrm{i}\pi}{a}\left[A^*_\alpha(\kappa)\frac{\partial A_\beta}{\partial\kappa} + B^*_\alpha(\kappa)\frac{\partial B_\beta}{\partial\kappa}\right]. \tag{A.14}$$

Substitution of equations (A.11), (A.12) and (A.13) into equation (A.14) then yields

$$X_{1,1}(\kappa) = X_{2,2}(\kappa) = 0, \qquad X_{1,2}(\kappa) = \mathrm{i}\Phi(\kappa), \qquad X_{2,1}(\kappa) = -\mathrm{i}\Phi(\kappa), \tag{A.15}$$

where we have set

$$\Phi(\kappa) = \frac{\pi}{a}\left(B_1\frac{\partial A_1}{\partial\kappa} - A_1\frac{\partial B_1}{\partial\kappa}\right) = \frac{J\delta\sin(\kappa a)}{\epsilon^2(\kappa)}. \tag{A.16}$$

The scattering matrices G and S are obtained after solving equations (A.6) and (A.7) in the two semi-cycles of oscillations $(0, T/2)$ and $(T/2, T)$, respectively. It can be shown that the simple relation $S = G^{\mathrm{T}}$ holds, where T denotes matrix transposition, i.e. $S_{\alpha,\beta} = G_{\beta,\alpha}$. In fact, for an ac force satisfying the symmetry constraint $F(T - t) = -F(t)$, taking into account equations (A.15) and that $E_2(\kappa) = -E_1(\kappa)$, integration of equations (A.6) and (A.7) backward in time, from $t = T$ to $t = T/2$, yields

$$\begin{pmatrix} -f_2(T/2) \\ f_1(T/2) \end{pmatrix} = G\begin{pmatrix} -f_2(T) \\ f_1(T) \end{pmatrix}. \tag{A.17}$$

Since $\det G = 1$, from equation (A.17) after inversion it readily follows that $S = G^{\mathrm{T}}$. For the parameter values used in figures 4(a) and (b) (square-wave modulation), the scattering matrix G is given by $G_{11} = -0.4232 + 0.5672\mathrm{i}$, $G_{12} = -0.7065$, $G_{21} = -G_{12}$, and $G_{22} = G^*_{11}$, whereas for the parameter values used in figures 4(c) and (d) (sinusoidal modulation) one has $G_{11} = 0.3200 - 0.6338\mathrm{i}$, $G_{12} = -0.7042$, $G_{21} = -G_{12}$, and $G_{22} = G^*_{11}$.

References

[1] Callaway J 1974 *Quantum Theory of the Solid State* (New York: Academic) pp 465–78
[2] Waschke C, Roskos H G, Schwedler R, Leo K, Kurz H and Köhler K 1993 *Phys. Rev. Lett.* **70** 3319
[3] Ben Dahan M, Peik E, Reichel J, Castin Y and Salomon C 1996 *Phys. Rev. Lett.* **76** 4508
[4] Wilkinson S R, Bharucha C F, Madison K W, Niu Q and Raizen M G 1996 *Phys. Rev. Lett.* **76** 4512
[5] Anderson B P and Kasevich M A 1998 *Science* **282** 1686
[6] Morandotti R, Peschel U, Aitchison J S, Eisenberg H S and Silberberg Y 1999 *Phys. Rev. Lett.* **83** 4756
[7] Pertsch T, Dannberg P, Elflein W, Bräuer A and Lederer F 1999 *Phys. Rev. Lett.* **83** 4752
[8] Trompeter H, Pertsch T, Lederer F, Michaelis D, Streppel U, Bräuer A and Peschel U 2006 *Phys. Rev. Lett.* **96** 023901
[9] Sanchis-Alepuz H, Kosevich Y A and Sanchez-Dehesa J 2007 *Phys. Rev. Lett.* **98** 134301
[10] Dunlap D H and Kenkre V M 1986 *Phys. Rev.* B **34** 3625
[11] Holthaus M 1992 *Phys. Rev. Lett.* **69** 351
[12] Dignam M M and de Sterke C M 2002 *Phys. Rev. Lett.* **88** 046806
[13] Madison K W, Fischer M C, Diener R B, Niu Q and Raizen M G 1998 *Phys. Rev. Lett.* **81** 5093
[14] Lignier H, Sias C, Ciampini D, Singh Y, Zenesini A, Morsch O and Arimondo E 2007 *Phys. Rev. Lett.* **99** 220403
[15] Eckardt A, Holthaus M, Lignier H, Zenesini A, Ciampini D, Morsch O and Arimondo E 2009 *Phys. Rev.* A **79** 013611
[16] Longhi S, Marangoni M, Lobino M, Ramponi R, Laporta P, Cianci E and Foglietti V 2006 *Phys. Rev. Lett.* **96** 243901
[17] Iyer R, Aitchison J S, Wan J, Dignam M M and de Sterke C M 2007 *Opt. Express* **15** 3212
[18] Szameit A, Garanovich I L, Heinrich M, Sukhorukov A A, Dreisow F, Pertsch T, Nolte S, Tünnermann A and Kivshar Y S 2009 *Nature Phys.* **5** 271
[19] Haller E, Hart R, Mark M J, Danzl J G, Reichsöllner L and Nägerl H C 2010 *Phys. Rev. Lett.* **104** 200403
[20] Witthaut D 2010 *Phys. Rev.* A **82** 033602
[21] Mülken O and Bauer M 2011 *Phys. Rev.* E **83** 061123
[22] Breid B M, Witthaut D and Korsch H J 2006 *New J. Phys.* **8** 110
[23] Breid B M, Witthaut D and Korsch H J 2007 *New J. Phys.* **9** 62
[24] Witthaut D, Trimborn F, Kegel V and Korsch H J 2011 *Phys. Rev.* A **83** 013609
[25] Longhi S 2006 *Europhys. Lett.* **76** 416
[26] Arevalo E and Morales-Molina L 2011 *Europhys. Lett.* **96** 60011
[27] Ding S and Wang G P 2012 *Appl. Phys. Lett.* **100** 151913
[28] Dreisow F, Szameit A, Heinrich M, Pertsch T, Nolte S, Tünnermann A and Longhi S 2009 *Phys. Rev. Lett.* **102** 076802
[29] Kling S, Salger T, Grossert C and Weitz M 2010 *Phys. Rev. Lett.* **105** 215301
[30] Longhi S 2008 *Phys. Rev. Lett.* **101** 193902
[31] Kempe J 2003 *Contemp. Phys.* **44** 307
[32] Venegas-Andraca S E 2012 arXiv:1201.4780
[33] Ryan C A, Laforest M, Boileau J C and Laflamme R 2005 *Phys. Rev.* A **72** 062317
[34] Schmitz H, Matjeschk R, Schneider Ch, Glueckert J, Enderlein M, Huber T and Schaetz T 2009 *Phys. Rev. Lett.* **103** 090504
[35] Zähringer F, Kirchmair G, Gerritsma R, Solano E, Blatt R and Roos C F 2010 *Phys. Rev. Lett.* **104** 100503
[36] Karski M, Förster L, Choi J-M, Steffen A, Alt W, Meschede D and Widera A 2009 *Science* **325** 174
[37] Knight P L, Roldan E and Sipe J E 2003 *Phys. Rev.* A **68** 020301

[38] Knight P L, Roldan E and Sipe J E 2003 *Opt. Commun.* **227** 147
[39] Francisco D, Iemmi C, Paz J P and Ledesma S 2006 *Phys. Rev.* A **74** 052327
[40] Zou X, Dong Y and Guo G 2006 *New J. Phys.* **8** 81
[41] Perets H B, Lahini Y, Pozzi F, Sorel M, Morandotti R and Silberberg Y 2008 *Phys. Rev. Lett.* **100** 170506
[42] Peruzzo A *et al* 2010 *Science* **329** 1500
[43] Sansoni L, Sciarrino F, Vallone G, Mataloni P, Crespi A, Ramponi R and Osellame R 2012 *Phys. Rev. Lett.* **108** 010502
[44] Schreiber A, Cassemiro K N, Potocek V, Gabris A, Mosley P J, Andersson E, Jex I and Silberhorn Ch 2010 *Phys. Rev. Lett.* **104** 050502
[45] Schreiber A, Cassemiro K N, Potocek V, Gabris A, Jex I and Silberhorn Ch 2011 *Phys. Rev. Lett.* **106** 180403
[46] Schreiber A, Gabris A, Rohde P P, Laiho K, Stefanak M, Potocek V, Hamilton C, Jex I and Silberhorn Ch 2012 *Science* **336** 55
[47] Oka T, Konno N, Arita R and Aoki H 2005 *Phys. Rev. Lett.* **94** 100602
[48] Dür W, Raussendorf R, Kendon V M and Briegel H-J 2002 *Phys. Rev.* A **66** 052319
[49] Eckert K, Mompart J, Birkl G and Lewenstein M 2005 *Phys. Rev.* A **72** 012327
[50] Cote R, Russell A, Eyler E E and Gould P L 2006 *New J. Phys.* **6** 156
[51] Joo J, Knight P L and Pachos J K 2007 *J. Mod. Opt.* **54** 1627
[52] Satapathy N, Hagman H, Zelan M, Kastberg A and Ramachandran H 2009 *Phys. Rev.* A **80** 012302
[53] Omar Y, Paunkovic N, Sheridan L and Bose S 2006 *Phys. Rev.* A **74** 042304